Free Radical Biology and Medicine ∎ (∎∎∎∎) ∎∎∎–∎∎∎

Contents lists available at ScienceDirect

Free Radical Biology and Medicine

journal homepage: www.elsevier.com/locate/freeradbiomed

Original Contribution

Osthole improves an accelerated focal segmental glomerulosclerosis model in the early stage by activating the Nrf2 antioxidant pathway and subsequently inhibiting NF-κB-mediated COX-2 expression and apoptosis

Shun-Min Yang [a], Yi-Lin Chan [a], Kuo-Feng Hua [b], Jia-Ming Chang [c], Hui-Ling Chen [c], Yung-Jen Tsai [c], Yu-Juei Hsu [d], Louis Kuoping Chao [e], Yang Feng-Ling [f], Yu-Ling Tsai [g], Shih-Hsiung Wu [f], Yih-Fuh Wang [h], Change-Ling Tsai [h], Ann Chen [a], Shuk-Man Ka [i,*]

[a] Department of Pathology and National Defense Medical Center, Taipei 114, Taiwan, Republic of China
[b] Department of Biotechnology and Animal Science, National Ilan University, Ilan, Taiwan, Republic of China
[c] Institute for Drug Evaluation Platform, Development Center for Biotechnology, Taipei, Taiwan, Republic of China
[d] Division of Nephrology, Department of Internal Medicine, Tri-Service General Hospital; National Defense Medical Center, Taipei 114, Taiwan, Republic of China
[e] Department of Cosmeceutics, China Medical University, Taichung, Taiwan, Republic of China
[f] Institute of Biological Chemistry, Academia Sinica, Taipei, Taiwan, Republic of China
[g] Graduate Institute of Life Sciences; and National Defense Medical Center, Taipei 114, Taiwan, Republic of China
[h] Graduate Institute of Electrical Engineering and Computer Science, National Penghu University of Science and Technology, Penghu, Taiwan, Republic of China
[i] Graduate Institute of Aerospace and Undersea Medicine, School of Medicine; National Defense Medical Center, Taipei 114, Taiwan, Republic of China

ARTICLE INFO

Article history:
Received 15 December 2013
Received in revised form
3 May 2014
Accepted 6 May 2014

Keywords:
Accelerated focal segmental glomerulosclerosis
Osthole
Renoprotective
Glomerular epithelial hyperplasia lesions
Periglomerular inflammation
Glomerular hyalinosis/sclerosis
Reactive oxygen species
COX-2
Apoptosis
Nrf2 pathway
Free radicals

ABSTRACT

Inflammatory reactions and oxidative stress are implicated in the pathogenesis of focal segmental glomerulosclerosis (FSGS), a common chronic kidney disease with relatively poor prognosis and unsatisfactory treatment regimens. Previously, we showed that osthole, a coumarin compound isolated from the seeds of *Cnidium monnieri*, can inhibit reactive oxygen species generation, NF-κB activation, and cyclooxygenase-2 expression in lipopolysaccharide-activated macrophages. In this study, we further evaluated its renoprotective effect in a mouse model of accelerated FSGS (acFSGS), featuring early development of proteinuria, followed by impaired renal function, glomerular epithelial cell hyperplasia lesions (a sensitive sign that precedes the development of glomerular sclerosis), periglomerular inflammation, and glomerular hyalinosis/sclerosis. The results show that osthole significantly prevented the development of the acFSGS model in the treated group of mice. The mechanisms involved in the renoprotective effects of osthole on the acFSGS model were mainly a result of an activated Nrf2-mediated antioxidant pathway in the early stage (proteinuria and ischemic collapse of the glomeruli) of acFSGS, followed by a decrease in: (1) NF-κB activation and COX-2 expression as well as PGE_2 production, (2) podocyte injury, and (3) apoptosis. Our data support that targeting the Nrf2 antioxidant pathway may justify osthole being established as a candidate renoprotective compound for FSGS.

Focal segmental glomerulosclerosis (FSGS)[1] is a very common category of chronic kidney disease and clinically features heavy proteinuria or nephrotic syndrome, with a relatively high frequency of progression to chronic renal failure and uremia [1–3]. The recurrence rate of FSGS has been reported in a high percentage of patients after renal transplantation [4]. Clinically, corticosteroids, some cytotoxic agents, and cyclosporin A have been commonly used in the treatment of patients with the renal disease [5–7], but both unsatisfactory effects on prevention of the progression of renal lesions [8,9] and various side effects for the

Abbreviations: acFSGS, accelerated focal segmental glomerulosclerosis; BUN, urea nitrogen; Col-IV, collagen IV; COX-2, cyclooxygenase-2; Cr, creatinine; Ccr, creatinine clearance; DHE, dihydroethidium; EPHL, glomerular epithelial cell hyperplasia lesion; FSGS, focal segmental glomerulosclerosis; GPx, glutathione peroxidase; HO-1, heme oxygenase 1; IHC, immunohistochemistry; Nrf2, nuclear factor E2-related factor 2; PGE_2, prostaglandin E_2; RLU, luminescence units; ROS, reactive oxygen species; TLC, thin-layer chromatography

* Corresponding author. Fax: +886 2 6600 0309.
E-mail addresses: shukmanka@gmail.com, mariaka@ndmctsgh.edu.tw (S.-M. Ka).

http://dx.doi.org/10.1016/j.freeradbiomed.2014.05.009
0891-5849/

patients [10–12] are still considered major concerns. Thus, seeking new agents with sufficient therapeutic effects and lowest toxicity/other systemic side effects becomes clinically important.

Inflammatory responses with mononuclear leukocyte recruitment [13,14], via the cyclooxygenase pathway [15,16], to oxidative stress [17,18], and in the form of apoptosis [19,20] have been implicated in the development and progression of FSGS, although the exact pathogenic mechanisms and etiological events remain largely unclear. Production of reactive oxygen species (ROS) and nitric oxide (NO) and reduced antioxidant capacity [18,21,22] contribute to the generation of oxidative stress, which can cause necrosis, inflammation, apoptosis, and fibrosis in the kidney [18,23,24]. Inhibition of oxidative stress prevents renal fibrosis by checking pathways of inflammation and apoptosis [18,24,25]. Furthermore, nuclear factor E2-related factor 2 (Nrf2), a transcription factor, can potently induce the production of antioxidants and prevent oxidative stress generation in chronic renal failure [26,27], renal inflammation [24,28], and renal fibrosis [18,29,30]. These effects involve mechanistic pathways such as binding of Nrf2 to antioxidant-response elements in the promoter region of a number of genes encoding antioxidant and phase 2 enzymes, including heme oxygenase 1 (HO-1), NAD(P)H quinone oxidoreductase 1, glutathione peroxidase (GPx), catalase, and superoxide dismutase [31,32].

Osthole, a coumarin compound, isolated from *Cnidium monnieri* (L.) Cusson seeds, which are used as a traditional Chinese medicine, has recently been shown to be anti-inflammatory [33–36], antiapoptotic [37,38], and antifibrotic [39,40]. In a recent paper, we demonstrated that the activation of NF-κB and production of ROS and cyclooxygenase-2 (COX-2) in macrophages were significantly reduced by osthole administration [35]. On the basis of its anti-inflammatory and antioxidant effects, we tested the hypothesis that osthole may prevent the development of renal lesions in an accelerated mouse model of FSGS (acFSGS). Our data justify osthole as being a potential renoprotective compound for FSGS and a new source for the development of therapeutic agents against FSGS.

Materials and methods

Osthole preparation and detection

Osthole was isolated from the *C. monnieri* (L.) Cusson seeds as described previously [35]. A mixture of dimethyl formamide, Tween 80, and saline was used as the solvent for osthole. Serum and urine levels of osthole in mice were determined using thin-layer chromatography (TLC; silica gel 60 F254, Merck, Boston, MA, USA) and MALDI–mass spectroscopy (MicroMax, Waters, CA, USA), respectively. Briefly, 1 μl serum, 1 μl urine, or osthole standards (50 ng–31.250 μg) were loaded onto the Silica G-60 TLC gel and then separated by the solvent system as *n*-hexane/ethyl acetate (7/3), and the R_f of osthole was equal to 0.5. The results were visible under UV light. Our preliminary tests showed that osthole, at more than 50 ng, could be detected by TLC analysis. Meanwhile, we used ethyl acetate to concentrate the osthole in serum and urine samples; briefly, 200 μl serum or urine was mixed with 200 μl ethyl acetate, and the ethyl acetate fraction was isolated and dried. Then, the concentrated samples were dissolved in 10 μl *n*-hexane/ethyl acetate and 1 μl was subjected to both silica G-60 TLC and MALDI–mass spectroscopy.

Establishment of the acFSGS model and experimental protocol

Experiments were performed on 8-week-old female BALB/c mice. Mice were intravenously injected with a single dose of adriamycin (0.1 mg/10 g body wt) to induce an acFSGS model [41], characterized by (1) early development of proteinuria, followed by impaired renal function; (2) glomerular epithelial cell hyperplasia lesions (EPHLs) that precede the development of glomerular sclerosis; (3) periglomerular mononuclear leukocyte infiltration; and (4) glomerular hyalinosis/sclerosis. Starting from 6 h before adriamycin injection, a group of mice was administered osthole at a daily dose of 30 mg/kg body wt by intraperitoneal injection or RTA402 (Selleckchem, Boston, MA, USA), an Nrf2 activator [42–44], at a daily dose of 2 mg/kg body wt by gavage until the day of sacrifice. Age- and sex-matched BALB/c mice injected intravenously with normal saline were used as normal controls, whereas FSGS mice given vehicle by intraperitoneal injection were used as disease controls. Urine samples were collected in metabolic cages on days 3, 7, 14, 21, and 28. Mice were killed at day 7 or 28 after disease induction. Body weight and kidney weight were measured. Renal cortical tissue and blood samples were collected and stored appropriately until analyses were executed. Urine protein levels were determined as described previously [18]. Serum samples were used to measure serum levels of blood urea nitrogen (BUN) and creatinine (Cr) [18], and creatinine clearance (Ccr) was determined by use of both serum Cr and urine Cr levels [45]. All animal experiments were performed with the ethical approval of the Institutional Animal Care and Use Committee of The National Defense Medical Center, Taiwan, and according to the ethical rules in the NIH *Guide for the Care and Use of Laboratory Animals*.

Renal pathology

Formalin-fixed and paraffin-embedded renal sections were prepared for renal pathologic evaluation and renal lesions scored as described previously [18]. For evaluations of ischemic collapse of the glomerular tuft, EPHLs, glomerular hyalinosis/sclerosis, and periglomerular inflammation at least 50 glomeruli in renal tissue sections were examined for each animal. The number of glomeruli with EPHLs was expressed as a percentage of the total number of evaluated glomeruli as described previously [41]. Meanwhile, renal sections were stained with Sirius red, a histochemical analysis for fibrosis (mainly for collagen I, II, and III), under a polarizing microscope as previously described [42,43].

For immunohistochemistry (IHC), formalin-fixed and paraffin-embedded renal sections were prepared and incubated with primary antibodies against mouse F4/80 (monocyte/macrophage; Serotec, Raleigh, NC, USA), pNF-κB p65 (Cell Signaling Technology, Danvers, MA, USA), collagen IV (Col-IV; Southern Biotech, Birmingham, AL, USA), or desmin (Lab Vision, Fremont, CA, USA) and then with biotinylated second antibodies (Dako, Carpinteria, CA, USA) and avidin–biotin–peroxidase complex (Dako). For detection of apoptosis, TUNEL was used. Formalin-fixed tissue sections were stained using a kit (ApopTag Plus Peroxidase in situ Apoptosis Detection kit; Chemicon, Temecula, CA, USA) according to the manufacturer's instructions. For scoring of staining of Sirius red and Col-IV, a quantitative image analysis software (Pax-it; Paxcam, Villa Park, IL, USA) was used as previously described. Briefly, 20 glomeruli were randomly selected from each section and positive signals within the selected glomerulus were highlighted, measured, and quantified as percentage positive area of the entire glomerulus. The numbers of phosphorylated NF-κB p65-, F4/80-, desmin- (a biomarker of podocyte injury), or TUNEL-positive cells were also determined by Pax-it software.

ROS determination

Renal ROS levels were measured by (1) dihydroethidium (DHE) binding, the fluorescence being quantified by counting the

Please cite this article as: Yang, S-M; et al. Osthole improves an accelerated focal segmental glomerulosclerosis model in the early stage by activating the Nrf2.... *Free Radic. Biol. Med.* (2014), http://dx.doi.org/10.1016/j.freeradbiomed.2014.05.009

percentage of the total nuclei that were positive per kidney cross section, and (2) a luminescence assay for superoxide anion levels, the results being represented as reactive luminescence units (RLU) per 15 min per milligram dry weight (i.e., RLU/15 min/mg dry wt), both as described previously [18]. Meanwhile, serum superoxide anion levels were measured by the luminescence assay above, the results being represented as RLU/15 min/ml.

Measurement of nuclear Nrf2 and cytosolic GPx activity in renal tissues

The activity of nuclear Nrf2 was evaluated using Trans-AM ELISA kits (Active Motif, Tokyo, Japan) according to the manufacturer's instructions. GPx activity in renal tissues was measured using a commercial glutathione peroxidase assay kit (Cayman Chemical, Ann Arbor, MI, USA) according to the manufacturer's instructions. Enzymatic activity was represented as a value relative to the protein concentration in renal homogenates.

Western blot analysis of Nrf2, COX-2, and caspases

Cytoplasmic and nuclear proteins were extracted from renal tissues using a Nuclear Extract Kit (Active Motif) according to the manufacturer's instructions. Target proteins were detected by Western blot analysis using antibodies against mouse Nrf2 (Santa Cruz Biotechnology, Dallas, TX, USA), COX-2 (Santa Cruz Biotechnology), and caspase-3, caspase-8, and caspase-9 (all from Cell Signaling Technology, Beverly, MA, USA) as described previously [30,34]. Antibodies to histone 3 (Cell Signaling Technology) for nuclear target proteins or β-actin (Santa Cruz Biotechnology) for cytosolic target proteins were used as internal controls.

Measurement of prostaglandin E_2 (PGE_2) and HO-1

Serum levels of PGE_2 and renal levels of HO-1 were measured using commercial ELISA kits (R&D Systems, Minneapolis, MN, USA), according to the manufacturer's instructions.

Measurement of nuclear Nrf2 in mesangial cells

Murine mesangial cells (CRL 1927; 1×10^6) were incubated for 0.5 h with 50 μM osthole or 100 nM RTA402 (Selleckchem) and then for 24 h with or without 2 μg/ml lipopolysaccharide (LPS), as described previously [34]. The protein levels of nuclear Nrf2 were evaluated by Trans-AM ELISA kits (Active Motif) described as above.

Data analysis

The results are presented as the mean ± SEM. Comparisons among groups were performed using one-way ANOVA, with post hoc correction by Tukey's method. A p value less than 0.05 was considered statistically significant.

Results

Osthole improves proteinuria, renal function, and renal lesions

AcFSGS mice treated with vehicle (vehicle + acFSGS mice) showed increased urine protein levels from day 7 after induction of FSGS that continued to increase to the end of the study at day 28 (all, $p < 0.05$) (Fig. 1A). However, this effect was significantly suppressed in FSGS mice treated with osthole (osthole + acFSGS mice), the levels being similar to those in normal control mice. With regard to renal function, significantly increased serum levels of BUN ($p < 0.005$; Fig. 1B) and Cr ($p < 0.005$; Fig. 1C) on day 28 were observed in vehicle + acFSGS mice, compared to those of normal control mice. This effect was greatly suppressed in osthole + acFSGS mice showing renal function similar to that of normal controls. There was no significant difference in BUN or Cr levels between normal control mice, vehicle + acFSGS mice, and osthole + acFSGS mice on day 7. In addition, the levels of Ccr were significantly increased in osthole + acFSGS mice on days 7 ($p < 0.05$) and 28 ($p < 0.005$), compared to those of vehicle + acFSGS mice (Fig. 1D). No significant changes in body weight (19.6 ± 1.0 g) or in kidney weight (0.18 ± 0.06 g) were observed in osthole + acFSGS mice, compared to vehicle + acFSGS (body weight, 18.7 ± 1.4 g; kidney weight, 0.19 ± 0.08 g) or normal control (body weight, 20.2 ± 0.5 g; kidney weight, 0.17 ± 0.04 g), on day 28. Unexpectedly, there were no osthole signals detectable in serum and urine samples by TLC or MALDI–mass spectroscopy in osthole + acFSGS mice under the experimental conditions of this study. We infer that osthole might convert into another structure when it enters the circulation of the treated mice, or the concentrations of osthole in serum and urine were below the detectable levels in the two analyses.

By light microscopy, on day 7, ischemic collapse of the glomerular tuft, diffuse in distribution, was identified in vehicle + acFSGS mice and persisted until day 28, but osthole + acFSGS mice showed a great improvement (day 7, $p < 0.005$; day 28, $p < 0.05$; Fig. 1E and F). Compared with normal control mice, vehicle + acFSGS mice on day 28 exhibited significantly increased percentages of glomeruli containing EPHLs ($p < 0.005$), segmental glomerular hyalinosis/sclerosis ($p < 0.005$), and periglomerular mononuclear leukocyte infiltration ($p < 0.005$) (Fig. 1E and G–I), but this effect was significantly prevented in osthole + acFSGS mice (each, $p < 0.01$; Fig. 1E and G–I). Furthermore, Sirius red staining showed significantly reduced levels of fibrosis within the glomerular tuft and in the periglomerular region on both days 7 and 28 in osthole + acFSGS mice compared to vehicle + acFSGS mice (Fig. 1J–L). As demonstrated by IHC, greatly increased renal expression levels of Col-IV on day 28 were seen in vehicle + acFSGS mice compared to normal control mice, but, again, this effect was suppressed in osthole + acFSGS (Fig. 1M–O).

Osthole enhances nuclear Nrf2 protein levels, cytosolic protein levels of HO-1, and GPx activity and reduces ROS production

Osthole is an antioxidant and free radical scavenger. First, we measured nuclear Nrf2 protein levels, cytosolic protein levels of HO-1, and GPx activity to evaluate the effects of osthole on the Nrf2 antioxidant signaling pathway in renal tissues. Osthole + acFSGS mice showed a marked increase in nuclear levels of Nrf2 protein as early as day 7 ($p < 0.01$) and levels remained high on day 28 ($p < 0.01$), compared to vehicle + acFSGS mice (Fig. 2A and B). Moreover, renal Nrf2 activity was greatly increased in osthole + acFSGS and RTA402-treated acFSGS (RTA402 + acFSGS) mice as early as day 7 (osthole + acFSGS, $p < 0.01$; RTA402 + acFSGS, $p < 0.005$) and persisted to day 28 (both $p < 0.005$), compared to vehicle + acFSGS mice (Fig. 2C). There was no significant difference in renal Nrf2 activity between osthole + acFSGS and RTA402 + acFSGS mice. Similarly, as shown in Fig. 2D, significantly increased renal levels of HO-1 were seen in osthole + acFSGS and RTA402 + acFSGS mice on both days 7 (both $p < 0.05$) and 28 (both $p < 0.005$), compared to vehicle + acFSGS mice, although there was no difference in the renal levels of the protein between osthole + acFSGS and RTA402 + acFSGS mice. Next, osthole + acFSGS mice tended to show an increase in renal GPx activity on day 7, although there was no statistical difference compared to vehicle + acFSGS mice ($p = 0.07$; Fig. 2E). In addition, a marked increase in renal GPx activity was observed in both osthole + acFSGS and RTA402 + acFSGS mice compared to vehicle + acFSGS mice on day 28 (both p

Please cite this article as: Yang, S-M; et al. Osthole improves an accelerated focal segmental glomerulosclerosis model in the early stage by activating the Nrf2.... *Free Radic. Biol. Med.* (2014), http://dx.doi.org/10.1016/j.freeradbiomed.2014.05.009

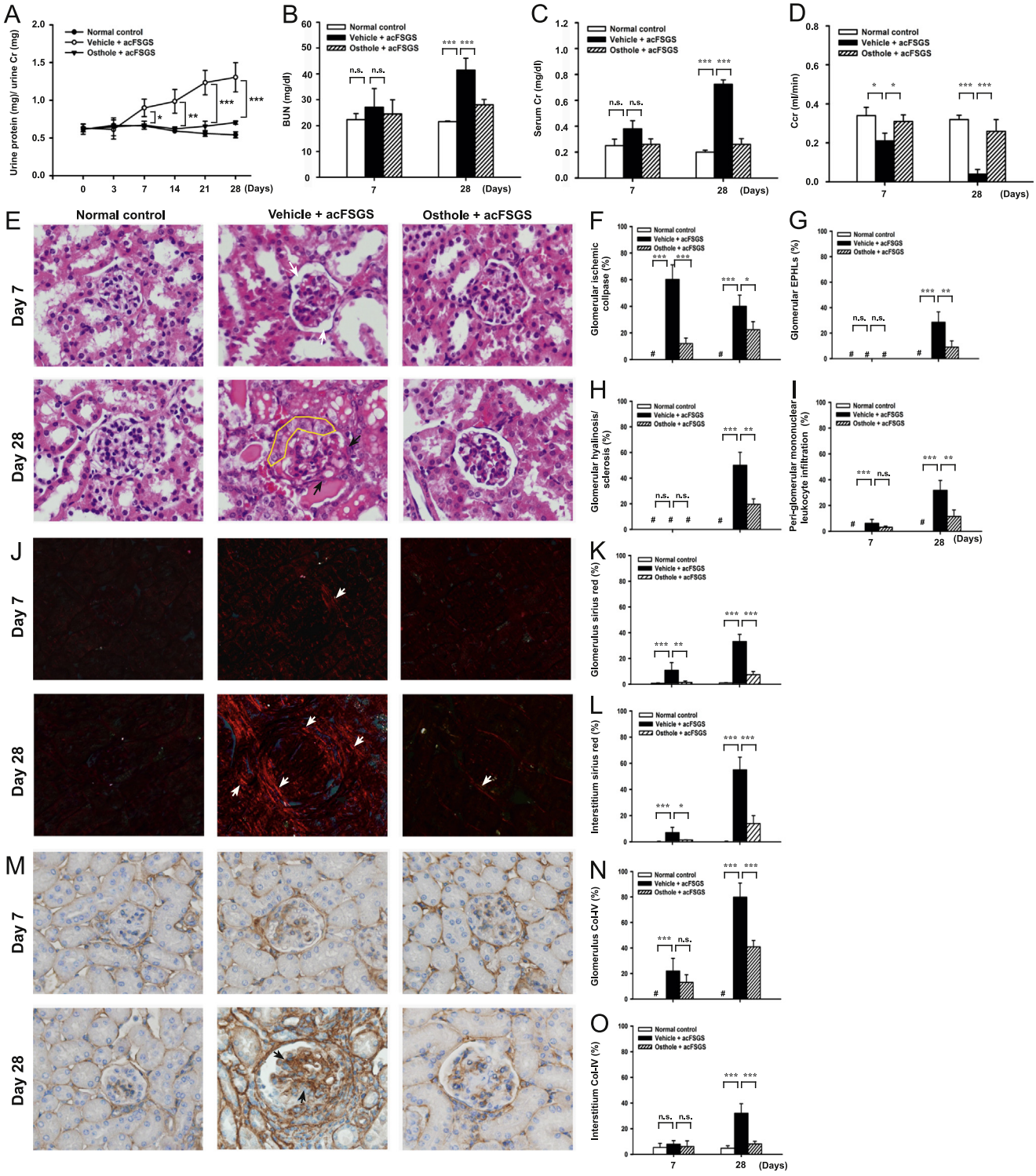

Fig. 1. Proteinuria, renal function, and renal histopathology. (A) Urine protein time-course study on days 3, 7, 14, 21, and 28. (B) Serum BUN levels, (C) serum Cr levels, and (D) Ccr on days 7 and 28. (E) Renal histopathology on days of 7 and 28 during treatment. H&E staining; original magnification each, 400 ×. The white arrows indicate ischemic collapse of the glomerulus; black arrows indicate glomerular hyalinosis/sclerosis; the yellow line indicates EPHLs. Scoring of (F) glomerular ischemic collapse, (G) glomerular EPHLs, (H) glomerular hyalinosis/sclerosis, or (I) periglomerular inflammation is shown on the right. (J) Sirius red staining (stained in red, as indicated by white arrows). (M) IHC for Col-IV. Scoring for (K, L) Sirius red staining or (N, O) Col-IV is shown on the right. Original magnification each, 400 ×. $^{*}p < 0.05$, $^{**}p < 0.01$, $^{***}p < 0.005$; n.s., not significant; #, not detectable.

< 0.005; Fig. 2E). No significant difference in renal GPx activity was observed between osthole + acFSGS and RTA402 + acFSGS mice. We further evaluated the effects of osthole in enhancing Nrf2 activity in LPS-primed mesangial cells. The results show that although significantly decreased Nrf2 activity was seen in LPS-primed mesangial cells compared to mesangial cells in saline (normal control), osthole restored the Nrf2 activity in the LPS-primed mesangial cells to the levels near RTA402-treated LPS-primed mesangial cells and normal controls (Fig. 2F).

We then examined the production levels of ROS. As demonstrated by DHE detection in renal tissues, on days 7 and 28, vehicle + acFSGS mice showed a marked increase in nuclear DHE levels of

Please cite this article as: Yang, S-M; et al. Osthole improves an accelerated focal segmental glomerulosclerosis model in the early stage by activating the Nrf2.... *Free Radic. Biol. Med.* (2014), http://dx.doi.org/10.1016/j.freeradbiomed.2014.05.009

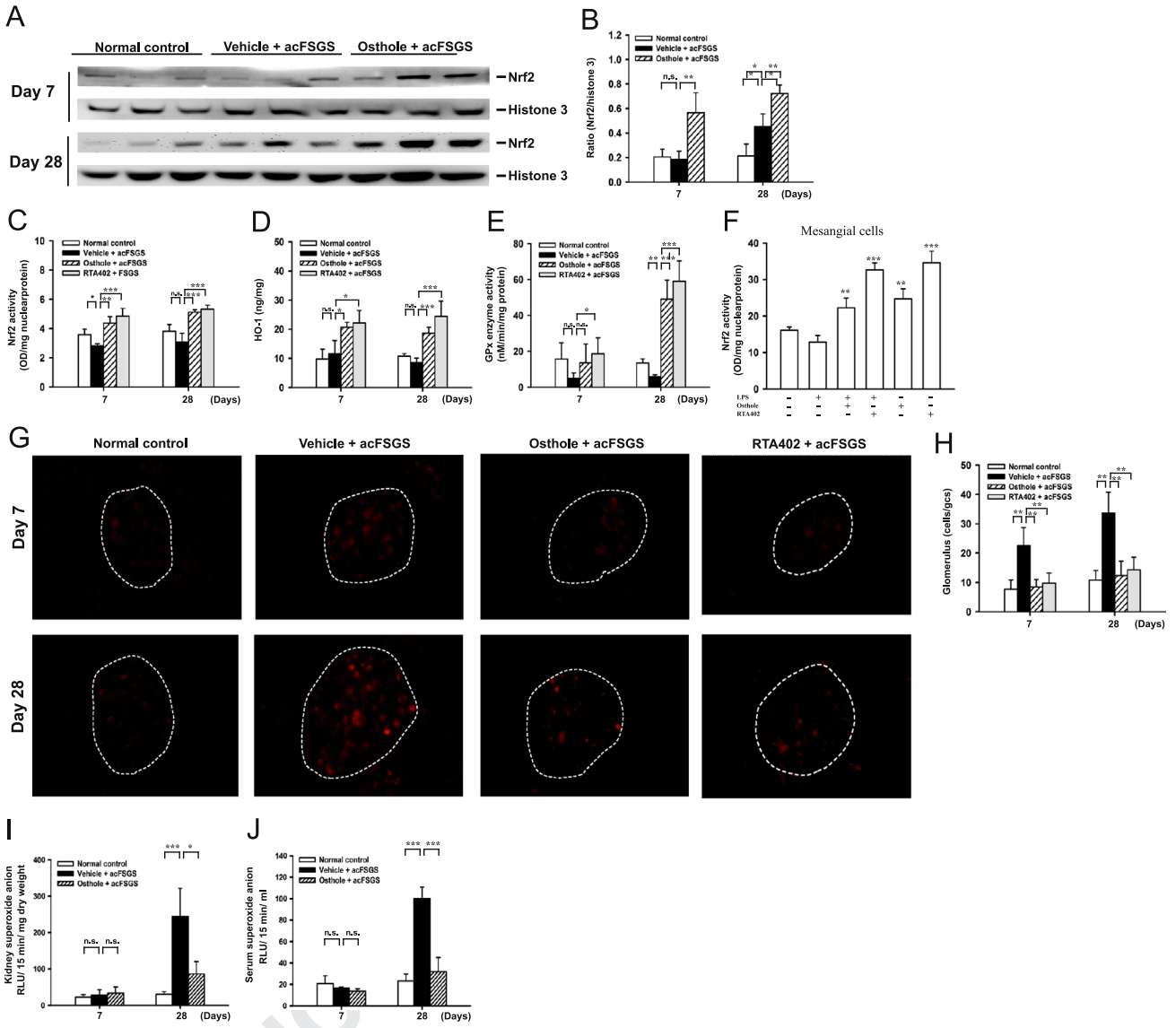

Fig. 2. Nuclear Nrf2 protein levels, cytosolic protein levels of HO-1, GPx activity, and ROS levels. (A) Representative Western blots for nuclear Nrf2 and (B) Nrf2/histone 3 ratio. (C) Renal nuclear Nrf2 activity. (D) Renal cytosolic HO-1 levels. (E) Renal cytosolic GPx activity. (F) Mesangial cell nuclear Nrf2 activity. (G) Kidney in situ ROS production demonstrated by DHE detection. (H) Scoring of nuclear DHE levels. ROS levels in (I) renal tissue and (J) serum. The dotted line circles indicate glomerulus, original magnification, 400×. $^{*}p < 0.05$, $^{**}p < 0.01$, $^{***}p < 0.005$. n.s., not significant.

the glomerulus, compared to normal control mice (both $p < 0.01$), but this effect was significantly inhibited in both osthole + acFSGS and RTA402 + acFSGS mice (all $p < 0.01$; Fig. 2G and H). By luminescence assay, as shown in Fig. 2I, renal superoxide anion levels of vehicle + acFSGS mice were greatly increased on day 28 compared to normal control mice ($p < 0.005$), but osthole administration significantly decreased superoxide anion levels to a level similar to that seen in normal control mice ($p < 0.05$). There was no such inhibitory effect on renal superoxide anion levels of the osthole + acFSGS mice on day 7. In addition, serum superoxide anion levels in vehicle + acFSGS mice were significantly increased on day 28 compared to normal control mice ($p < 0.005$), but this effect was greatly inhibited by osthole administration ($p < 0.005$; Fig. 2J).

Osthole inhibits renal macrophage infiltration, nuclear translocation of NF-κB, and COX-2 expression and reduces serum levels of PGE_2

Renal inflammatory responses have been involved in the pathogenesis of FSGS. First, we detected renal inflammation, NF-κB-mediated COX-2 expression in renal tissue, and serum levels of PGE_2. As shown in Fig. 3A–C, macrophage ($F4/80^{+}$) infiltration mainly in the periglomerular region of the interstitium was seen on day 28 of vehicle + acFSGS mice ($p < 0.005$) and this effect was greatly reduced by osthole administration ($p < 0.005$). We then investigated the effects of osthole on NF-κB activation in renal tissues. As shown in Fig. 3D–F, vehicle + acFSGS mice showed significantly increased NF-κB p65 nuclear translocation compared to normal control mice on day 28 ($p < 0.005$) and this effect was significantly inhibited in osthole + acFSGS mice ($p < 0.005$). To validate the involvement of COX-2 in the NF-κB-mediated inflammatory pathway, we measured renal levels of COX-2 expression. As shown in Fig. 3G and H, renal COX-2 levels were greatly elevated in vehicle + acFSGS mice compared to normal control mice in renal tissues on day 28 ($p < 0.005$), and this effect was significantly inhibited in osthole + acFSGS mice ($p < 0.005$). We further determined serum levels of PGE_2, a downstream molecule of COX-2, in the mice, and osthole + acFSGS mice showed significantly reduced serum levels of PGE_2 ($p < 0.005$) compared to vehicle + acFSGS mice showing markedly increased serum levels of PGE_2 on day 28 compared to normal control mice

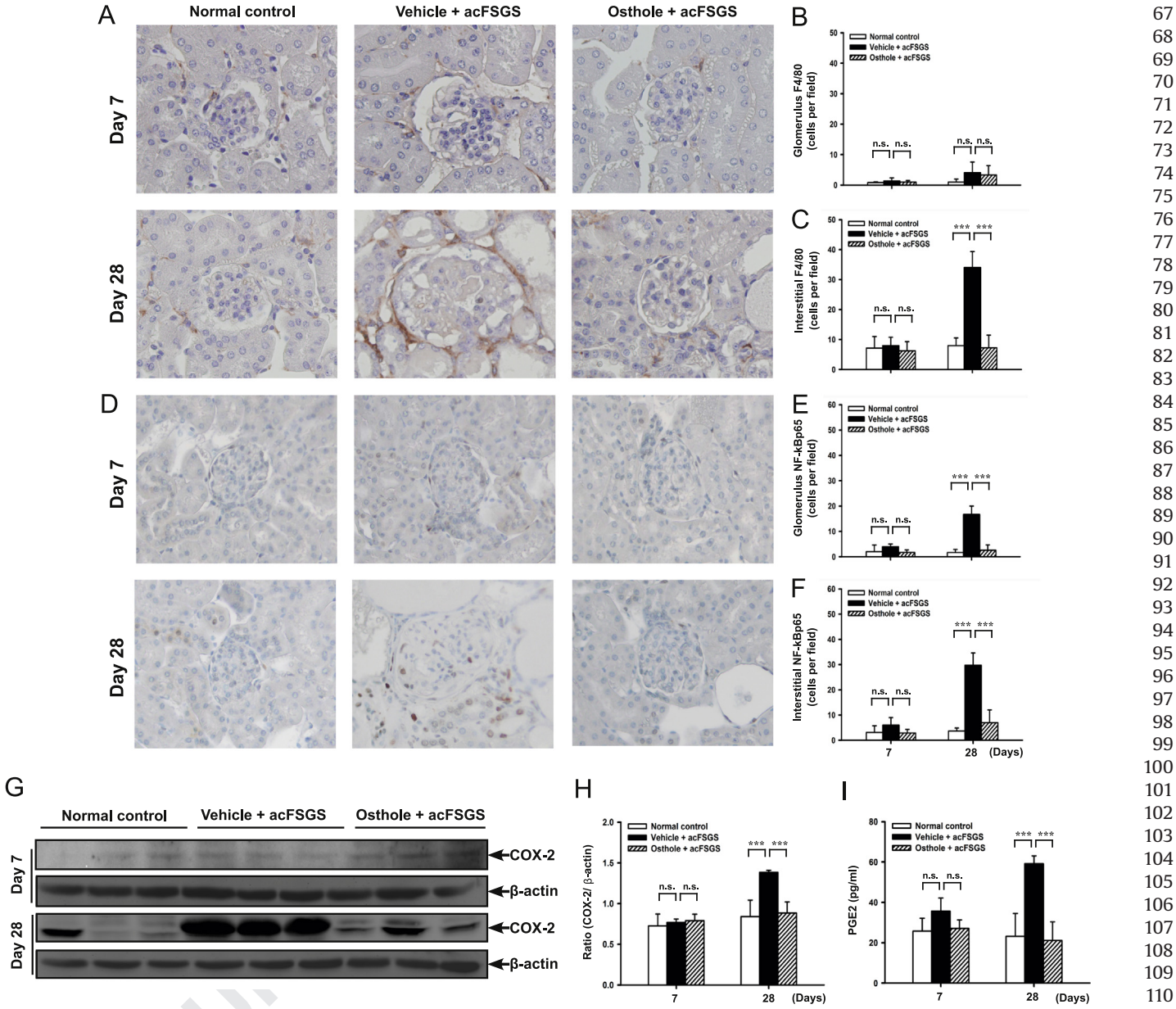

Fig. 3. Renal macrophage infiltration and activation of NF-κB pathway. Detection of (A–C) F4/80 monocytes/macrophages and (D–F) NF-κB p65 by immunohistochemical staining. Original magnification, 400 ×. The scoring for the glomerulus and interstitium of F4/80 (B, C) or NF-κB p65 staining (E, F) is shown on the right. (G) Representative Western blots of COX-2 in renal tissues and (H) COX-2/β-actin ratio. (I) PGE_2 levels in serum by enzyme-linked immunosorbent assay. ***$p < 0.005$. n.s., not significant.

($p < 0.005$; Fig. 3I). There was no detectable difference in macrophage infiltration, NF-κB activation, COX-2 expression, and PGE_2 levels between the vehicle + acFSGS, osthole + acFSGS, and normal control mice on day 7.

Osthole prevents podocyte injury and renal apoptosis

Damage to podocytes has been implicated in the development of glomerular sclerosis [44,45]. As shown in Fig. 4A and B, although vehicle + acFSGS mice showed greatly increased numbers of podocytes that expressed desmin (a biomarker of podocyte injury) compared to normal control mice ($p < 0.01$), this effect was significantly inhibited in osthole + acFSGS mice ($p < 0.05$). In addition, an increased number of podocytes and renal tubular epithelial cells with apoptosis was seen in vehicle + acFSGS mice on day 28 compared to normal control mice and this effect was significantly inhibited by osthole administration, as demonstrated by TUNEL staining ($p < 0.005$; Fig. 4C–E). In a further analysis of the pathway of apoptosis, the renal levels of caspase-3, caspase-8, and caspase-9 were determined. As shown in Fig. 4F and G, the levels of the mature forms of renal caspase-3 (p17 fragments) ($p < 0.01$) and caspase-9 (p37 fragments) ($p < 0.005$) were increased in vehicle + acFSGS mice, compared to normal control mice on day 28. However, this effect was significantly inhibited in osthole + acFSGS mice (both, $p < 0.01$). There was no detectable difference in renal levels of caspase-8 between vehicle + acFSGS, osthole + acFSGS, and normal control mice (data not shown). These data support that inhibition of the intrinsic pathway of apoptosis was involved in the renoprotective effects of osthole in the treated mice.

Discussion

In this study, osthole, a pure compound isolated from *C. monnieri* (L.) Cusson seeds, was found to modulate the acFSGS model by preventing proteinuria, renal function disturbance,

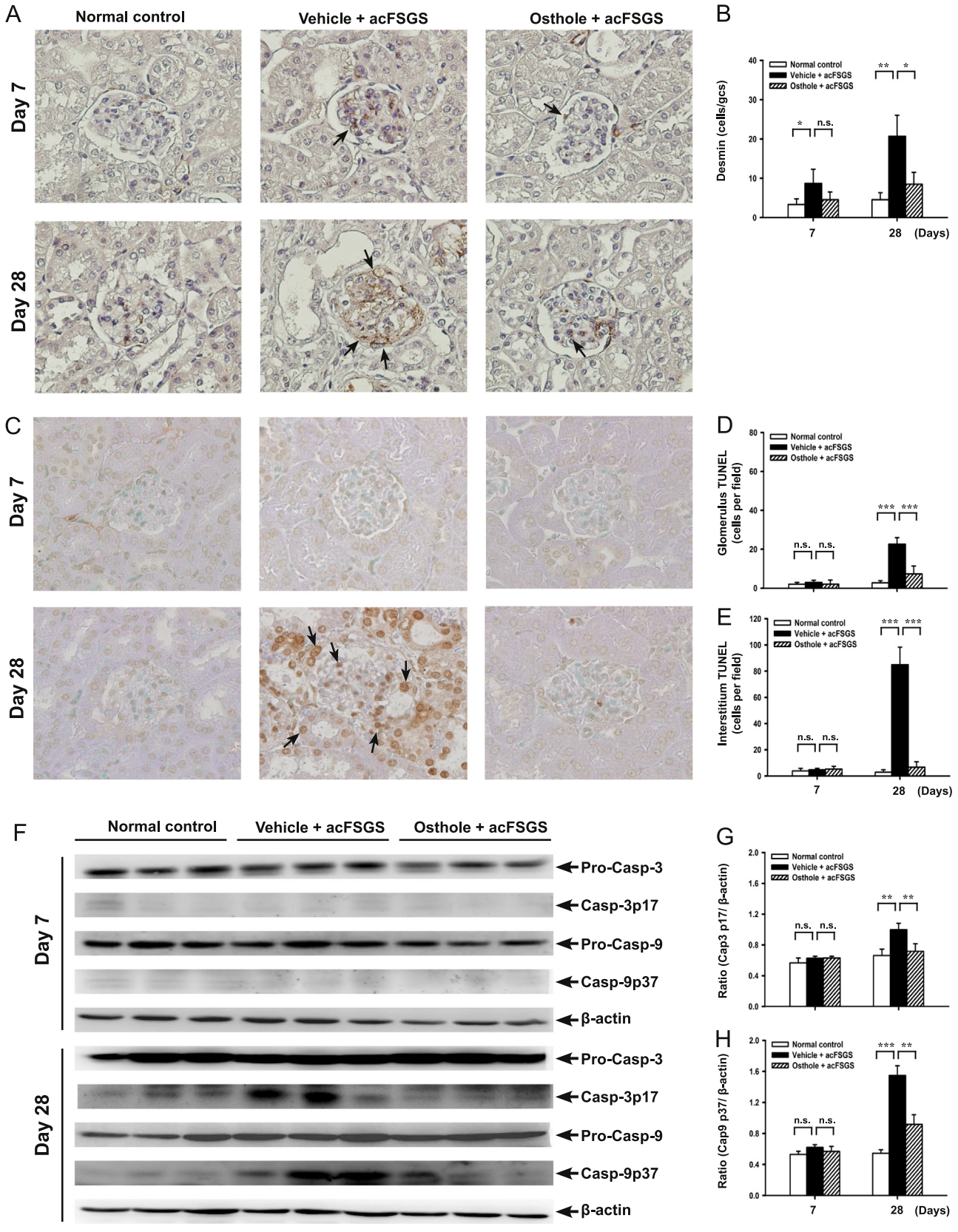

Fig. 4. Podocyte injury and renal apoptosis. (A) Immunohistochemical staining for desmin expression in the glomerulus, reflecting injury of podocytes (black arrows). (B) Scoring of desmin expression in renal tissue by IHC staining. (C) TUNEL staining. Original magnification each, 400 ×. Scoring of TUNEL-positive cells in (D) glomerulus and (E) renal tubule. (F) Representative Western blots for renal procaspase-3 and procaspase-9. Ratio of (G) active caspase-3/β-actin and (H) active caspase-9/β-actin. $^{*}p < 0.05$, $^{**}p < 0.01$, $^{***}p < 0.005$. n.s., not significant.

Please cite this article as: Yang, S-M; et al. Osthole improves an accelerated focal segmental glomerulosclerosis model in the early stage by activating the Nrf2.... *Free Radic. Biol. Med.* (2014), http://dx.doi.org/10.1016/j.freeradbiomed.2014.05.009

EPHLs, periglomerular mononuclear leukocyte infiltration, and glomerular hyalinosis/sclerosis. Activation of the Nrf2 antioxidant pathway in the early stage (proteinuria and ischemic collapse of the glomeruli) of acFSGS, followed by inhibited NF-κB activation and COX-2 expression, was involved in the renoprotective effects of osthole in this acFSGS model of mice.

In our previous studies [18,24,34] and others [46], the Nrf2 signaling pathway serves as a crucial antioxidant mechanism in various renal disorders. In the present study, we showed that osthole administration activated the Nrf2 signaling pathway as early as day 7 after the induction of disease in association with increased expression of HO-1 (Fig. 2D) and GPx (Fig. 2E), both of which are its downstream molecules, although suppression of the NF-κB-mediated COX-2 pathway was observed later on day 28 (Fig. 3G–I). In this potential mechanism, the NF-κB-mediated inflammatory pathway can upregulate the expression of COX-2 [47]. Overexpression of COX-2 has been implicated in various types of renal inflammation [23,48,49] and can increase susceptibility to podocyte injury [50,51], which is an evolutional pathological feature of FSGS [52,53]. In this study, we showed that osthole: (1) inhibited mononuclear leukocyte infiltration and COX-2 expression and PGE_2 production, downstream of the NF-κB-mediated inflammatory pathway (Fig. 3, and (2) prevented podocyte injury as demonstrated by decreased desmin expression (Fig. 4A and B) and apoptosis (Fig. 4C–E), in renal tissues of osthole + acFSGS mice on day 28, suggesting that osthole rendered its beneficial effects on this acFSGS model in the established stage of renal lesions by inhibiting the NF-κB-mediated inflammatory response involving COX-2 expression in the kidney.

In addition, our data showed that osthole increased the expression levels of Nrf2 and HO-1, but decreased NF-κB activation and reduced the expression levels of COX-2 and PGE_2. NF-κB is one of the most important regulators of inflammatory gene expression including COX-2 [58]. Inhibition of NF-κB reduces COX-2 expression induced by various stimuli [59–61]; thus we suggested that osthole-mediated downregulation of COX-2 and PGE_2 is due to NF-κB inhibition. The question is whether osthole-mediated Nrf2 activation is responsible for the NF-κB inhibition. Previous studies showed that Nrf2 negatively regulates NF-κB activation as evidenced by inhibition of Nrf2 significantly enhancing NF-κB transcriptional activity and NF-κB-dependent gene expression [62,63]. Upregulation of the Nrf2 downstream molecule HO-1 also inhibits NF-κB activation [64]. In addition, upregulation of Nrf2 improves lupus nephritis by reducing NF-κB activation and by neutralizing reactive oxygen species generation [65]. In addition, Nrf2-induced expression of antiapoptotic molecules such as Bcl-2 has been shown to enhance cell survival and drug resistance [54,55]. Apoptosis plays a pathogenic role in the development and progression of FSGS [19,38]. In agreement with this notion, we showed that only mild renal pathology (Figs. 1F–I and 4A–E) was observed in the kidney of osthole + acFSGS mice associated with enhanced renal activation of Nrf2 expression (Fig. 2A–C). Also, osthole administration resulted in the prevention of apoptosis in renal cells (Fig. 4A–E) and reduced levels of activated caspase-3 and caspase-9 in renal tissues (Fig. 4F–H). Our data suggest that inhibition of renal apoptosis of the intrinsic pathway may contribute to the beneficial effects of osthole on the acFSGS model. In this regard, Zheng et al. [38] and our recent report [34] also showed that osthole is renoprotective in mouse models of renal disorders via either antiapoptosis or anti-inflammatory mechanisms. All together, our results provide evidence to support osthole being considered as a candidate renoprotective compound, although the pharmacological activities, exact mode of action, and toxicity need to be further investigated. However, COX-2 has also been shown to be antiapoptotic in renal medullary interstitial cells [56] and mesangial cells [57]. Obviously, these findings may rebut a direct antiapoptotic effect of osthole in our study. In this regard, the cyclooxygenase pathway has also been shown to be involved in glomerular injury in patients with FSGS [16], and overexpression of COX-2 can incite podocyte injury in a mouse model of FSGS [15]. Cheng et al. [54] further showed that overexpression of podocyte COX-2 increases susceptibility to podocyte injury, although basal COX-2 may be important for podocyte survival, partly by activation of the thromboxane receptor. Nevertheless, further investigation is necessary to dissect the exact mechanisms by which osthole administration conferred its effects in preventing the development and evolution of the acFSGS model.

In agreement with the data from the mice above, we also observed that osthole could significantly enhance Nrf2 activities in LPS-primed mesangial cells (Fig. 2F), suggesting that one of the mechanisms involved in the renoprotective effects of osthole on the acFSGS was via activation of the Nrf2-mediated antioxidant pathway in the intrinsic cells of the glomerulus. On the other hand, in a recent report, Chen et al. [70] showed a protective role of osthole in acute lung injury caused by LPS and also showed the activation of Nrf2 by osthole, but did not show the exact role of Nrf2 in vivo. In the present study, it is important to discriminate the effect of osthole on suppression of LPS/Toll-like receptor-mediated NF-κB signaling from the possible protective role through Nrf2 activation with proper tools, especially including the use of Nrf2-knockout mice, in further investigations.

Uncited references

[66–69].

Acknowledgments

This study was supported by grants from the National Science Council (NSC102-2321-B-016-002), Medical Affairs Bureau (103-M012), and Tri-Service General Hospital (TSGH-C103-079), Taiwan, Republic of China.

References

[1] D'Agati, V. D.; Kaskel, F. J.; Falk, R. J. Focal segmental glomerulosclerosis. *N. Engl. J. Med.* **365:**2398–2411; 2011.
[2] Kiffel, J.; Rahimzada, Y.; Trachtman, H. Focal segmental glomerulosclerosis and chronic kidney disease in pediatric patients. *Adv. Chronic Kidney Dis.* **18:**332–-338; 2011.
[3] Rood, I. M.; Deegens, J. K.; Wetzels, J. F. Genetic causes of focal segmental glomerulosclerosis: implications for clinical practice. *Nephrol. Dial. Transplant.* **27:**882–890; 2012.
[4] Maas, R. J.; Deegens, J. K.; van den Brand, J. A.; Cornelissen, E. A.; Wetzels, J. F. A retrospective study of focal segmental glomerulosclerosis: clinical criteria can identify patients at high risk for recurrent disease after first renal transplantation. *BMC Nephrol.* **14:**47; 2013.
[5] Korbet, S. M. Treatment of primary FSGS in adults. *J. Am. Soc. Nephrol.* **23:**1769–1776; 2012.
[6] Nikibakhsh, A. A.; Mahmoodzadeh, H.; Karamyyar, M.; Hejazi, S.; Noroozi, M.; Macooie, A. A. Treatment of steroid and cyclosporine-resistant idiopathic nephrotic syndrome in children. *Int. J. Nephrol.* **2011:**930965; 2011.
[7] Xu, S.; Xu, G.; Zeng, L. Immunosuppressive treatment in primary focal segmental glomerulosclerosis. *J. Nephrol.* **25:**626–635; 2012.
[8] Braun, N.; Schmutzler, F.; Lange, C.; Perna, A.; Remuzzi, G.; Risler, T.; Willis, N. S. Immunosuppressive treatment for focal segmental glomerulosclerosis in adults. *Cochrane Database Syst. Rev.* **3:**CD003233; 2008.
[9] Troyanov, S.; Wall, C. A.; Miller, J. A.; Scholey, J. W.; Cattran, D. C., Toronto Glomerulonephritis Registry Group. Focal and segmental glomerulosclerosis: definition and relevance of a partial remission. *J. Am. Soc. Nephrol.* **16:**1061–-1068; 2005.
[10] Goumenos, D. S.; Tsagalis, G.; El Nahas, A. M.; Shortland, J. R.; Davlouros, P.; Vlachojannis, J. G.; Brown, C. B. Immunosuppressive treatment of idiopathic focal segmental glomerulosclerosis: a five-year follow-up study. *Nephron Clin. Pract.* **104:**c75–c82; 2006.

[11] Passerini, P.; Scolari, F.; Frasca, G. M.; Leoni, A.; Venturelli, C.; Dallera, N.; Ravera, S.; Balestra, E.; Freddi, P.; Fanciulli, E.; D'Arezzo, M.; Sagripanti, S. [Controversial issues in the Giornale Italiano di Nefrologia: how to treat patients with focal segmental glomerular sclerosis]. *G. Ital. Nefrol.* **26:**563–576; 2009.

[12] Stirling, C. M. Focal segmental glomerulosclerosis—does treatment work? *Nephron Clin. Pract.* **104:**c83–c84; 2006.

[13] Benz, K.; Buttner, M.; Dittrich, K.; Campean, V.; Dotsch, J.; Amann, K. Characterisation of renal immune cell infiltrates in children with nephrotic syndrome. *Pediatr. Nephrol.* **25:**1291–1298; 2010.

[14] D'Agati, V. Pathologic classification of focal segmental glomerulosclerosis. *Semin. Nephrol.* **23:**117–134; 2003.

[15] Cheng, H.; Wang, S.; Jo, Y. I.; Hao, C. M.; Zhang, M.; Fan, X.; Kennedy, C.; Breyer, M. D.; Moeckel, G. W.; Harris, R. C. Overexpression of cyclooxygenase-2 predisposes to podocyte injury. *J. Am. Soc. Nephrol.* **18:**551–559; 2007.

[16] McCarthy, E. T.; Sharma, M. Indomethacin protects permeability barrier from focal segmental glomerulosclerosis serum. *Kidney Int.* **61:**534–541; 2002.

[17] Kuo, H. T.; Kuo, M. C.; Chiu, Y. W.; Chang, J. M.; Guh, J. Y.; Chen, H. C. Increased glomerular and extracellular malondialdehyde levels in patients and rats with focal segmental glomerulosclerosis. *Eur. J. Clin. Invest.* **35:**245–250; 2005.

[18] Tsai, P. Y.; Ka, S. M.; Chao, T. K.; Chang, J. M.; Lin, S. H.; Li, C. Y.; Kuo, M. T.; Chen, P.; Chen, A. Antroquinonol reduces oxidative stress by enhancing the Nrf2 signaling pathway and inhibits inflammation and sclerosis in focal segmental glomerulosclerosis mice. *Free Radic. Biol. Med.* **50:**1503–1516; 2011.

[19] Erkan, E.; Garcia, C. D.; Patterson, L. T.; Mishra, J.; Mitsnefes, M. M.; Kaskel, F. J.; Devarajan, P. Induction of renal tubular cell apoptosis in focal segmental glomerulosclerosis: roles of proteinuria and Fas-dependent pathways. *J. Am. Soc. Nephrol.* **16:**398–407; 2005.

[20] Zhang, J.; Pippin, J. W.; Krofft, R. D.; Naito, S.; Liu, Z. H.; Shankland, S. J. Podocyte repopulation by renal progenitor cells following glucocorticoids treatment in experimental FSGS. *Am. J. Physiol. Renal Physiol.* **304:**F1375–-F1389; 2013.

[21] Ozbek, E. Induction of oxidative stress in kidney. *Int. J. Nephrol* **2012:**465897; 2012.

[22] Storz, P. Forkhead homeobox type O transcription factors in the responses to oxidative stress. *Antioxid. Redox Signal.* **14:**593–605; 2011.

[23] Aminzadeh, M. A.; Nicholas, S. B.; Norris, K. C.; Vaziri, N. D. Role of impaired Nrf2 activation in the pathogenesis of oxidative stress and inflammation in chronic tubulo-interstitial nephropathy. *Nephrol. Dial. Transplant.* **28:**2038–-2045; 2013.

[24] Yang, S. M.; Ka, S. M.; Hua, K. F.; Wu, T. H.; Chuang, Y. P.; Lin, Y. W.; Yang, F. L.; Wu, S. H.; Yang, S. S.; Lin, S. H.; Chang, J. M.; Chen, A. Antroquinonol mitigates an accelerated and progressive IgA nephropathy model in mice by activating the Nrf2 pathway and inhibiting T cells and NLRP3 inflammasome. *Free Radic. Biol. Med.* **61C:**285–297; 2013.

[25] Rojas-Rivera, J.; Ortiz, A.; Egido, J. Antioxidants in kidney diseases: the impact of bardoxolone methyl. *Int. J. Nephrol* **2012:**321714; 2012.

[26] Tapia, E.; Zatarain-Barron, Z. L.; Hernandez-Pando, R.; Zarco-Marquez, G.; Molina-Jijon, E.; Cristobal-Garcia, M.; Santamaria, J.; Pedraza-Chaverri, J. Curcumin reverses glomerular hemodynamic alterations and oxidant stress in 5/6 nephrectomized rats. *Phytomedicine* **20:**359–366; 2013.

[27] Thornalley, P. J.; Rabbani, N. Dietary and synthetic activators of the antistress gene response in treatment of renal disease. *J. Renal Nutr.* **22:**195–202; 2012.

[28] Soetikno, V.; Sari, F. R.; Lakshmanan, A. P.; Arumugam, S.; Harima, M.; Suzuki, K.; Kawachi, H.; Watanabe, K. Curcumin alleviates oxidative stress, inflammation, and renal fibrosis in remnant kidney through the Nrf2–Keap1 pathway. *Mol. Nutr. Food Res.* **57:**1649–1659; 2013.

[29] Oh, C. J.; Kim, J. Y.; Choi, Y. K.; Kim, H. J.; Jeong, J. Y.; Bae, K. H.; Park, K. G.; Lee, I. K. Dimethylfumarate attenuates renal fibrosis via NF-E2-related factor 2-mediated inhibition of transforming growth factor-beta/Smad signaling. *PLoS One* **7:**e45870; 2012.

[30] Yang, S. M.; Hua, K. F.; Lin, Y. C.; Chen, A.; Chang, J. M.; Kuoping Chao, L.; Ho, C. L.; Ka, S. M. Citral is renoprotective for focal segmental glomerulosclerosis by inhibiting oxidative stress and apoptosis and activating Nrf2 pathway in mice. *PLoS One* **8:**e74871; 2013.

[31] Guerrero-Beltran, C. E.; Calderon-Oliver, M.; Pedraza-Chaverri, J.; Chirino, Y. I. Protective effect of sulforaphane against oxidative stress: recent advances. *Exp. Toxicol. Pathol.* **64:**503–508; 2012.

[32] Pedruzzi, L. M.; Stockler-Pinto, M. B.; Leite Jr M.; Mafra, D. Nrf2–Keap1 system versus NF-kappaB: the good and the evil in chronic kidney disease? *Biochimie* **94:**2461–2466; 2012.

[33] Chao, X.; Zhou, J.; Chen, T.; Liu, W.; Dong, W.; Qu, Y.; Jiang, X.; Ji, X.; Zhen, H.; Fei, Z. Neuroprotective effect of osthole against acute ischemic stroke on middle cerebral ischemia occlusion in rats. *Brain Res.* **1363:**206–211; 2010.

[34] Hua, K. F.; Yang, S. M.; Kao, T. Y.; Chang, J. M.; Chen, H. L.; Tsai, Y. J.; Chen, A.; Yang, S. S.; Chao, L. K.; Ka, S. M. Osthole mitigates progressive IgA nephropathy by inhibiting reactive oxygen species generation and NF-kappaB/NLRP3 pathway. *PLoS One* **8:**e77794; 2013.

[35] Liao, P. C.; Chien, S. C.; Ho, C. L.; Wang, E. I.; Lee, S. C.; Kuo, Y. H.; Jeyashoke, N.; Chen, J.; Dong, W. C.; Chao, L. K.; Hua, K. F. Osthole regulates inflammatory mediator expression through modulating NF-kappaB, mitogen-activated protein kinases, protein kinase C, and reactive oxygen species. *J. Agric. Food Chem.* **58:**10445–10451; 2010.

[36] Zheng, Y.; Lu, M.; Ma, L.; Zhang, S.; Qiu, M.; Ma, X. Osthole ameliorates renal ischemia–reperfusion injury by inhibiting inflammatory response. *Urol. Int.* **91:**350–356; 2013.

[37] Okamoto, T.; Kawasaki, T.; Hino, O. Osthole prevents anti-Fas antibody-induced hepatitis in mice by affecting the caspase-3-mediated apoptotic pathway. *Biochem. Pharmacol.* **65:**677–681; 2003.

[38] Zheng, Y.; Lu, M.; Ma, L.; Zhang, S.; Qiu, M.; Wang, Y. Osthole ameliorates renal ischemia–reperfusion injury in rats. *J. Surg. Res.* **183:**347–354; 2013.

[39] Chen, R.; Xue, J.; Xie, M. L. Reduction of isoprenaline-induced myocardial TGF-beta1 expression and fibrosis in osthole-treated mice. *Toxicol. Appl. Pharmacol.* **256:**168–173; 2011.

[40] Hou, X. H.; Cao, B.; Liu, H. Q.; Wang, Y. Z.; Bai, S. F.; Chen, H. Effects of osthole on apoptosis and TGF-beta1 of hypertrophic scar fibroblasts. *J. Asian Nat. Prod. Res.* **11:**663–669; 2009.

[41] Shui, H. A.; Ka, S. M.; Yang, S. M.; Lin, Y. F.; Lo, Y. F.; Chen, A. Osteopontin as an injury marker expressing in epithelial hyperplasia lesions helpful in prognosis of focal segmental glomerulosclerosis. *Transl. Res.* **150:**216–222; 2007.

[42] Pergola, P. E.; Raskin, P.; Toto, R. D.; Meyer, C. J.; Huff, J. W.; Grossman, E. B.; Krauth, M.; Ruiz, S.; Audhya, P.; Christ-Schmidt, H.; Wittes, J.; Warnock, D. G., BEAM Study Investigators. Bardoxolone methyl and kidney function in CKD with type 2 diabetes. *N. Engl. J. Med.* **365:**327–336; 2011.

[43] Wu, Q. Q.; Wang, Y.; Senitko, M.; Meyer, C.; Wigley, W. C.; Ferguson, D. A.; Grossman, E.; Chen, J.; Zhou, X. J.; Hartono, J.; Winterberg, P.; Chen, B.; Agarwal, A.; Lu, C. Y. Bardoxolone methyl (BARD) ameliorates ischemic AKI and increases expression of protective genes Nrf2, PPARgamma, and HO-1. *Am. J. Physiol. Renal Physiol.* **300:**F1180–F1192; 2011.

[44] Reisman, S. A.; Chertow, G. M.; Hebbar, S.; Vaziri, N. D.; Ward, K. W.; Meyer, C. J. Bardoxolone methyl decreases megalin and activates nrf2 in the kidney. *J. Am. Soc. Nephrol.* **23:**1663–1673; 2012.

[45] Dunn, S. R.; Qi, Z.; Bottinger, E. P.; Breyer, M. D.; Sharma, K. Utility of endogenous creatinine clearance as a measure of renal function in mice. *Kidney Int.* **65:**1959–1967; 2004.

[46] Junqueira, L. C.; Cossermelli, W.; Brentani, R. Differential staining of collagens type I, II and III by Sirius red and polarization microscopy. *Arch. Histol. Jpn.* **41:**267–274; 1978.

[47] Sund, S.; Grimm, P.; Reisaeter, A. V.; Hovig, T. Computerized image analysis vs semiquantitative scoring in evaluation of kidney allograft fibrosis and prognosis. *Nephrol. Dial. Transplant.* **19:**2838–2845; 2004.

[48] Kistler, A. D.; Singh, G.; Pippin, J.; Altintas, M. M.; Yu, H.; Fernandez, I. C.; Gu, C.; Wilson, C.; Srivastava, S. K.; Dietrich, A.; Walz, K.; Kerjaschki, D.; Ruiz, P.; Dryer, S.; Sever, S.; Dinda, A. K.; Faul, C.; Shankland, S. J.; Reiser, J. Transient receptor potential channel 6 (TRPC6) protects podocytes during complement-mediated glomerular disease. *J. Biol. Chem.* **288:**36598–36609; 2013.

[49] Wu, J.; Zheng, C.; Fan, Y.; Zeng, C.; Chen, Z.; Qin, W.; Zhang, C.; Zhang, W.; Wang, X.; Zhu, X.; Zhang, M.; Zen, K.; Liu, Z. Downregulation of microRNA-30 facilitates podocyte injury and is prevented by glucocorticoids. *J. Am. Soc. Nephrol.* **25:**92–104; 2014.

[50] Ruiz, S.; Pergola, P. E.; Zager, R. A.; Vaziri, N. D. Targeting the transcription factor Nrf2 to ameliorate oxidative stress and inflammation in chronic kidney disease. *Kidney Int.* **83:**1029–1041; 2013.

[51] Li, W.; Khor, T. O.; Xu, C.; Shen, G.; Jeong, W. S.; Yu, S.; Kong, A. N. Activation of Nrf2–antioxidant signaling attenuates NFkappaB-inflammatory response and elicits apoptosis. *Biochem. Pharmacol.* **76:**1485–1489; 2008.

[52] Di Paola, R.; Genovese, T.; Impellizzeri, D.; Ahmad, A.; Cuzzocrea, S.; Esposito, E. The renal injury and inflammation caused by ischemia–reperfusion are reduced by genetic inhibition of TNF-alphaR1: a comparison with infliximab treatment. *Eur. J. Pharmacol.* **700:**134–146; 2013.

[53] Ranganathan, P. V.; Jayakumar, C.; Mohamed, R.; Dong, Z.; Ramesh, G. Netrin-1 regulates the inflammatory response of neutrophils and macrophages, and suppresses ischemic acute kidney injury by inhibiting COX-2-mediated PGE2 production. *Kidney Int.* **83:**1087–1098; 2013.

[54] Cheng, H.; Fan, X.; Guan, Y.; Moeckel, G. W.; Zent, R.; Harris, R. C. Distinct roles for basal and induced COX-2 in podocyte injury. *J. Am. Soc. Nephrol.* **20:**1953–-1962; 2009.

[55] Jo, Y. I.; Cheng, H.; Wang, S.; Moeckel, G. W.; Harris, R. C. Puromycin induces reversible proteinuric injury in transgenic mice expressing cyclooxygenase-2 in podocytes. *Nephron Exp. Nephrol.* **107:**e87–e94; 2007.

[56] D'Agati, V. D. Podocyte injury in focal segmental glomerulosclerosis: lessons from animal models (a play in five acts). *Kidney Int.* **73:**399–406; 2008.

[57] Guo, J.; Ananthakrishnan, R.; Qu, W.; Lu, Y.; Reiniger, N.; Zeng, S.; Ma, W.; Rosario, R.; Yan, S. F.; Ramasamy, R.; D'Agati, V.; Schmidt, A. M. RAGE mediates podocyte injury in adriamycin-induced glomerulosclerosis. *J. Am. Soc. Nephrol.* **19:**961–972; 2008.

[58] Tak, P. P.; Firestein, G. S. NF-kappaB: a key role in inflammatory diseases. *J. Clin. Invest.* **107:**7–11; 2001.

[59] Crofford, L. J.; Tan, B.; McCarthy, C. J.; Hla, T. Involvement of nuclear factor kappa B in the regulation of cyclooxygenase-2 expression by interleukin-1 in rheumatoid synoviocytes. *Arthritis Rheum.* **40:**226–236; 1997.

[60] D'Acquisto, F.; Iuvone, T.; Rombola, L.; Sautebin, L.; Di Rosa, M.; Carnuccio, R. Involvement of NF-kappaB in the regulation of cyclooxygenase-2 protein expression in LPS-stimulated J774 macrophages. *FEBS Lett.* **418:**175–178; 1997.

[61] Lin, C. C.; Hsieh, H. L.; Shih, R. H.; Chi, P. L.; Cheng, S. E.; Yang, C. M. Up-regulation of COX-2/PGE2 by endothelin-1 via MAPK-dependent NF-kappaB pathway in mouse brain microvascular endothelial cells. *Cell Commun. Signaling* **11:**8; 2013.

[62] Thimmulappa, R. K.; Lee, H.; Rangasamy, T.; Reddy, S. P.; Yamamoto, M.; Kensler, T. W.; Biswal, S. Nrf2 is a critical regulator of the innate immune response and survival during experimental sepsis. *J. Clin. Invest.* **116:**984–995; 2006.

Please cite this article as: Yang, S-M; et al. Osthole improves an accelerated focal segmental glomerulosclerosis model in the early stage by activating the Nrf2.... *Free Radic. Biol. Med.* (2014), http://dx.doi.org/10.1016/j.freeradbiomed.2014.05.009

[63] Hwang, Y. J.; Lee, E. W.; Song, J.; Kim, H. R.; Jun, Y. C.; Hwang, K. A. MafK positively regulates NF-kappaB activity by enhancing CBP-mediated p65 acetylation. *Sci. Rep.* **3:**3242; 2013.
[64] Bellezza, I.; Tucci, A.; Galli, F.; Grottelli, S.; Mierla, A. L.; Pilolli, F.; Minelli, A. Inhibition of NF-kappaB nuclear translocation via HO-1 activation underlies alpha-tocopheryl succinate toxicity. *J. Nutr. Biochem.* **23:**1583–1591; 2012.
[65] Jiang, T.; Tian, F.; Zheng, H.; Whitman, S. A.; Lin, Y.; Zhang, Z.; Zhang, N.; Zhang, D. D. Nrf2 suppresses lupus nephritis through inhibition of oxidative injury and the NF-kappaB-mediated inflammatory response. *Kidney Int.* **85:**333–343; 2014.
[66] Luna-Lopez, A.; Triana-Martinez, F.; Lopez-Diazguerrero, N. E.; Ventura-Gallegos, J. L.; Gutierrez-Ruiz, M. C.; Damian-Matsumura, P.; Zentella, A.; Gomez-Quiroz, L. E.; Konigsberg, M. Bcl-2 sustains hormetic response by inducing Nrf-2 nuclear translocation in L929 mouse fibroblasts. *Free Radic. Biol. Med.* **49:**1192–1204; 2010.
[67] Niture, S. K.; Jaiswal, A. K. Nrf2 protein up-regulates antiapoptotic protein Bcl-2 and prevents cellular apoptosis. *J. Biol. Chem.* **287:**9873–9886; 2012.
[68] Han, Q.; Zhang, X.; Xue, R.; Yang, H.; Zhou, Y.; Kong, X.; Zhao, P.; Li, J.; Yang, J.; Zhu, Y.; Guan, Y. AMPK potentiates hypertonicity-induced apoptosis by suppressing NFkappaB/COX-2 in medullary interstitial cells. *J. Am. Soc. Nephrol.* **22:**1897–1911; 2011.
[69] Miller, B.; Patel, V. A.; Sorokin, A. Cyclooxygenase-2 rescues rat mesangial cells from apoptosis induced by adriamycin via upregulation of multidrug resistance protein 1 (P-glycoprotein). *J. Am. Soc. Nephrol.* **17:**977–985; 2006.
[70] Chen, X. J.; Zhang, B.; Hou, S. J.; Shi, Y.; Xu, D. Q.; Wang, Y. X.; Liu, M. L.; Dong, H. Y.; Sun, R. H.; Bao, N. D.; Jin, F. G.; Li, Z. C. Osthole improves acute lung injury in mice by up-regulating Nrf-2/thioredoxin 1. *Respir. Physiol. Neurobiol.* **188:**214–222; 2013.

Please cite this article as: Yang, S-M; et al. Osthole improves an accelerated focal segmental glomerulosclerosis model in the early stage by activating the Nrf2.... *Free Radic. Biol. Med.* (2014), http://dx.doi.org/10.1016/j.freeradbiomed.2014.05.009